Two Element Dielectric Resonator Antenna with Beam Switching

M. Kamran Saleem, Majeed A. S. Alkanhal, and Abdel Fattah Sheta

Department of Electrical Engineering, College of Engineering
King Saud University, Riyadh, P. O. Box 800, 11421, Saudi Arabia
msaleem@ksu.edu.sa, majeed@ksu.edu.sa, asheta@ksu.edu.sa

Abstract **─** A wideband two element rectangular dielectric resonator antenna (DRA) is proposed in this paper. Each DRA element has two excitation strips and four parasitic patches. A wide impedance bandwidth of more than 37% at the center frequency of 1.6 GHz is achieved. The antenna radiation beam can be switched between two positions in elevation plane, i.e., θ = 45° and θ = -45°. The measured antenna gain is found to be more than 6 dB in the whole frequency band of operation. The matching and the radiation characteristics of the designed switched beam antenna are studied and validated by measurements. A very good agreement between the measured and simulated results is observed.

Index Terms **─** Dielectric resonator antenna, parasitic patch, switched beam antenna, wideband antenna.

I. INTRODUCTION

The dielectric resonator antenna (DRA) was first introduced by Long in 1983 [1]. The DRA has many advantages such as low dissipation loss, high radiation efficiency and ease of excitation as well as wider impedance bandwidth [2-4]. Different shapes of DRAs such as rectangular, cylindrical, hemispherical, elliptical and perforated have been presented in the literature [5-9]. The DRA's having rectangular shape offer advantages over hemispherical and cylindrical shaped DRAs since they are easy to fabricate and have more design flexibility. There are many different schemes for exciting DRA such as probe feed, helical feed, slot feed and strip line feed [10-12].

The beam switching antenna finds many uses in applications requiring tracking or interference mitigation. The beam switching can be achieved by physical movement of antenna or by electronic control of some antenna parameters [13]. The mechanically steerable antennas [14] may be difficult to implement since they require a motor to rotate the antenna structure. One of possible solutions is to use multiple feeds [15-17] and radiation pattern can be switched using electronic switches, but this multiple feed antenna structure requires extra circuitry (phase shifters, power splitters/combiners) for feed selection and multiple antenna elements, resulting in a more complex and a large antenna structure.

The work in this paper presents a two element small size DRA, which is investigated to achieve reconfigurable radiation patterns with high gain. The antenna impedance bandwidth is found to be 800 MHz (1.3 - 2.1 GHz). In addition, the antenna radiation pattern can be switched in two positions in elevation plan, i.e., at θ = 45° and θ = -45° from 1.3 to 1.9 GHz. The simulations are done using Ansys HFSS and a prototype is developed and tested to prove the design concept and to verify the simulation results.

II. THEORETICAL ANALYSIS

The analysis of operation of DRA is a complex electromagnetic field problem. The numerical techniques such as finite element method (FEM), finite-difference time domain (FDTD) and the method of moments (MoM) are usually employed to predict/compute the resonance frequency of DRA with specific dimensions. Since all these numerical techniques require intensive memory and processing, therefore, several simple models have been developed to estimate the resonance frequency of DRA. Utilizing the most commonly used the dielectric waveguide model (DWM), the TE_{mnl} resonance frequency (f_0) for rectangular DRA can be calculated as follows [18]:

$$f_0 = \frac{c}{2\pi\sqrt{\varepsilon_r}}\sqrt{k_x^2 + k_y^2 + k_z^2}, \quad (1)$$

$$k_x = \frac{m\pi}{a}, \quad (2)$$

$$k_z = \frac{l\pi}{2d}, \quad (3)$$

$$k_y \tan\left(\frac{k_y b}{2}\right) = \sqrt{(\varepsilon_r - 1)k_0^2 - k_y^2}, (n = 1), \quad (4)$$

$$k_x^2 + k_y^2 + k_z^2 = \varepsilon_r k_0^2, \quad (5)$$

where, k_0 is the free space wavenumber, c is the speed of light in vacuum and k_x, k_y and k_z are the wavenumber inside the DR in three directions. The ε_r is dielectric constant and a, b and d are length, width and height of DR respectively. The subscripts m, n and l of TE_{mnl}

Submitted On: November 13, 2014
Accepted On: August 14, 2015

denotes the number of extremes in the x, y and z directions respectively. Utilizing the above mentioned DWM the DR ($\varepsilon_r = 10$) size is found to be a = 32 mm, b = 29.6 mm, and d = 48.85 mm, resulting in the dominant TE_{111} mode resonance frequency to be at 1.84 GHz.

Furthermore, the selection of suitable coupling/excitation scheme is one of the most crucial parts of DRA design. The type and location of coupling/excitation scheme very effectively effect the DRA performance. We know from the electromagnetic theory and the Lorentz theorem of reciprocity [19] that the amount of coupling between the sources (electric or magnetic) and the fields inside the DRA can be determined by:

$$k \propto \int (E.J_e) dV, \tag{6}$$

$$k \propto \int (H.J_m) dV, \tag{7}$$

where, **E** and **H** are the electric and magnetic field intensity vectors. $\mathbf{J_e}$ and $\mathbf{J_m}$ are the electric and magnetic currents. The above equations state that in order to achieve strong coupling between an electric or magnetic current source and the DRA, the excitation source should be placed in regime of strongest electric or magnetic field of the DRA. In proposed DRA structure, the vertical probe excitation scheme is employed, which is considered as vertical electric current source. The most suitable location for this excitation scheme is at the middle of DRA broad side wall, since the electric field is maximum in this location. As mentioned in our pervious communication [20], the dual excitation scheme is employed to split the broad side radiation pattern into two lobes, which plays an important role in DRA beam switching.

III. ANTENNA DESIGN AND CONFIGURATION

The proposed two element DRA configuration is shown in Fig. 1. The dielectric resonators (DRs) have dielectric constant and dielectric loss tangent of 10 and 0.0005, respectively. As mentioned earlier, the DR size is selected to be a = 32 mm, b = 29.6 mm, and d = 48.85 mm. The DRs are placed over FR4 substrate of thickness 1.575 mm. The bottom side of the substrate is fully copper plated and acts as an antenna ground plane. The DR is excited by means of dual excitation strips placed at the middle of two opposite side walls in the YZ-plane. The excitation strip lengths and widths are L_E = 30 mm and W_E = 5.3 mm, respectively. Furthermore, four parasitic patches are placed at the corner of each DR side wall in the XZ-plane having length L_P = 22 mm and width W_P = 1.5 mm. Each parasitic patch is connected to the antenna ground plane through a metallic via hole in the FR4 substrate. To provide a short or open circuit between the parasitic patch and the antenna ground plane, a switch can be placed between them. All eight switches are shown in the top view of the proposed antenna structure as illustrated in Fig. 2. The optimum center to center distance between the two DR is found to be S = 108 mm ($0.6\lambda_0$, at center frequency of 1.6 GHz). The four excitation strips are connected together by means of a microstrip feed network and a coaxial probe is placed at the center of microstrip line of length L_3 = 109.48 mm and width T_2 = 1.48 mm. The microstrip feed network is optimized to mitigate the degradation caused in antenna return loss by the microstrip line in close proximity of DR [11]. The optimized dimensions shown in Fig. 2 are as follows: L_1 = 15 mm, L_2 = 45 mm, L_4 = 21.48 mm, T_1 = 0.74 mm, L = 235.6 mm and W = 144 mm.

The DRAs excited by a single feed usually has a maximum at broad side direction [18,21]. However, with the proposed dual strip excitation scheme the radiation pattern is altered such that a null in broadside direction is created and the main lobe is splitted into two lobes with maxima at approximately ±45° in elevation plane. Readers are referred to [20] to have a better understanding of DRA excitation utilizing dual excitation strips. The two parasitic patches on one side having connections with antenna ground plane through switches are utilized to suppress one of the lobes created, and thus provide pattern reconfigurability. Moreover, the dimensions of the parasitic patch also control the impedance bandwidth [20]. The antenna radiation pattern is found to be linearly polarized with the proposed arrangement of dual excitation strips and parasitic patches.

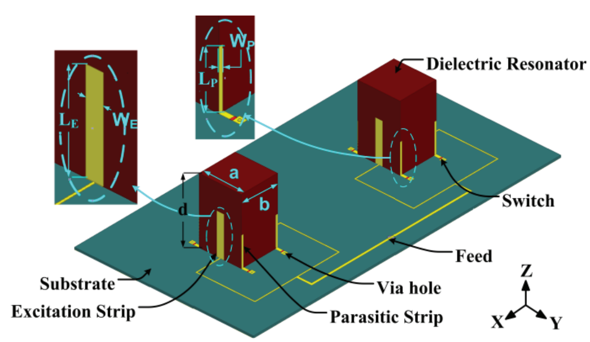

Fig. 1. The proposed two element DRA configuration. Each DRA has two excitation strips (YZ-plane) and four parasitic patches (XZ-plane).

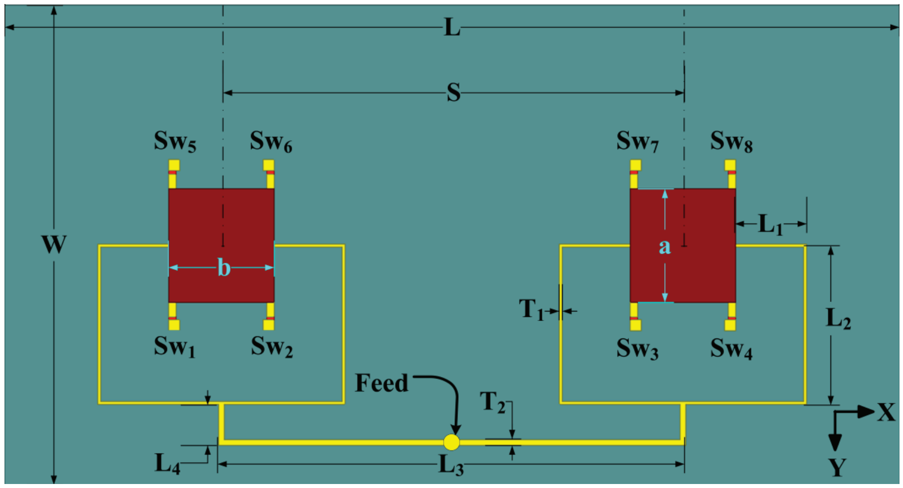

Fig. 2. Top view of two element DRA, with a = 32 mm, b = 29.6 mm, d = 48.85 mm, S = 108 mm, L_E = 30 mm, W_E = 5.3 mm, L_P = 22 mm, W_P = 1.5 mm, L_1 = 15 mm, L_2 = 45 mm, L_3 = 109.48 mm, L_4 = 21.48 mm, T_1 = 0.74 mm, T_2 = 0.74 mm L = 235.6 mm and W = 144 mm.

A prototype is fabricated to prove the design concept and to verify the simulations. The photograph of the fabricated antenna is shown in Fig. 3. The two DRs are glued over the FR4 substrate with a dielectric adhesive having dielectric constant of 10. The excitation strips and parasitic patches are cut from the conducting tap having thickness of 0.035 mm and positioned over the DR at appropriate locations as shown in Fig. 1. The utilization of eight switches (Sw_1 - Sw_8) in the proposed DRA configuration plays an important role to switch antenna radiation pattern in two directions in elevation plane (i.e., at θ = 45° and θ = -45°). Although there are many possible switching combinations, but only two cases are discussed, which are summarized in Table 1. The antenna radiation pattern is not controllable with cases other than mentioned in Table 1, where “OFF” state refers to an open circuit between corresponding parasitic patch and antenna ground plane, and “ON” state refers to a short circuit between corresponding parasitic patch and antenna ground plane. For the proof of concept the switches are hard wired on the prototype (i.e., a small piece of conducting copper tap is utilized to provide a short circuit between the parasitic patch and the antenna ground plane). Subsequently, the return loss and radiation pattern measurements are taken for the fabricated DRA antenna structure as revealed in the subsequent sections.

Table 1: Switch configuration for switching antenna radiation pattern in elevation plane

	ON		OFF	
CASE-I	SW_1, SW_3,	SW_2, SW_4	SW_5, SW_7,	SW_6, SW_8
CASE-II	SW_5, SW_7,	SW_6, SW_8	SW_1, SW_3,	SW_2, SW_4

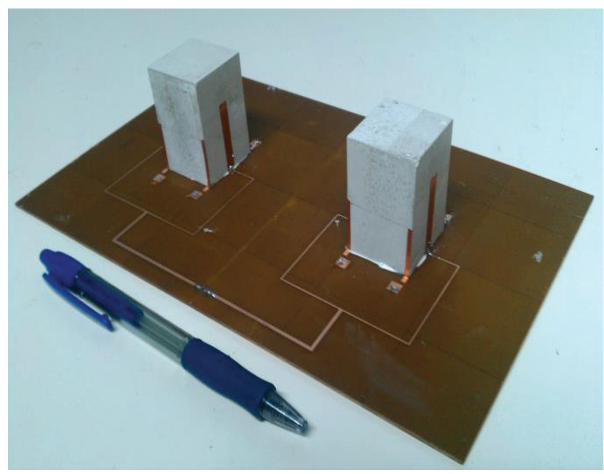

Fig. 3. Photograph of the developed two element DRA.

IV. SIMULATION AND MEASURED RESULTS

The DRA presented in Section II is simulated in Ansys HFSS. The simulated and measured return loss for the two cases mentioned in Table 1 are shown in Fig. 4. The overall antenna impedance bandwidth is found to be 800 MHz (1.3 - 2.1 GHz). The resonance of TE_{111} mode is found theoretically by DWM to be at 1.84 GHz. Experimentally, it is found at 1.78 GHz and corresponds to the strip loaded DR mode [21]. Furthermore, the resonance seen around 1.35 GHz is highly influenced by the length of the parasitic patch [20] and corresponds to the patch loaded DR mode [21]. The optimum length of the parasitic patch is found to be L_P = 22 mm. The field pattern inside DR is investigated and it is found that the antenna operates in a perturbed type TE_{111} from 1.3 - 1.9 GHz.

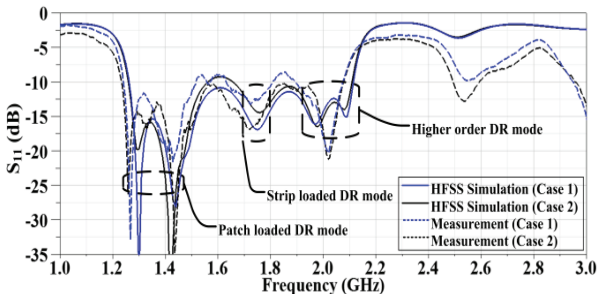

Fig. 4. Simulated and measured return loss (S_{11}) for two cases mentioned in Table 1.

The simulated 3D radiation patterns for both cases, i.e., Case-I and Case-II of Table 1 are shown in Fig. 5 for a better illustration of antenna beam switching. The comparison of measured and simulated radiation patterns at $\varphi = 90^{\circ}$ (YZ-plane) at various frequencies for Case-I and Case-II, mentioned in Table 1, are shown in Fig. 6 and Fig. 7, respectively. It is found that after 1.9 GHz the antenna radiation pattern cannot be switched efficiently. This may be attributed to the excitation of higher order modes such as TE_{112} and TE_{113}. Theoretically, these two modes are found to be at 2.05 GHz and 2.34 GHz, respectively. Therefore, the actual antenna bandwidth in which antenna radiation pattern can be switched is from 1.3 to 1.9 GHz. The measured gain at center frequency of 1.6 GHz is found to be 6.92 dB at $\theta = -45^{\circ}$ for Case-I and 6.71 dB at $\theta = 45^{\circ}$ for Case-II respectively. The measured gain of the two-element DRA for both cases remains above 6 dB in whole frequency band of operation and is shown in Fig. 8.

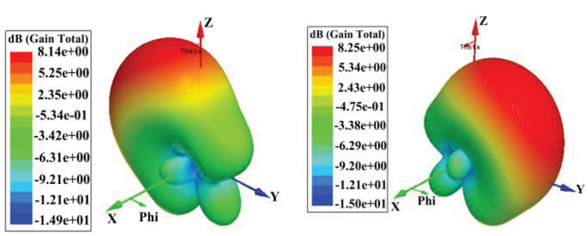

(a) (b)

Fig. 5. 3D radiation pattern at 1.6 GHz for Case-I and Case-II given in Table 1: (a) Case-I, and (b) Case-II.

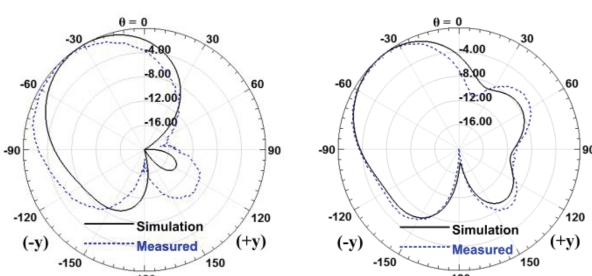

(a) (b)

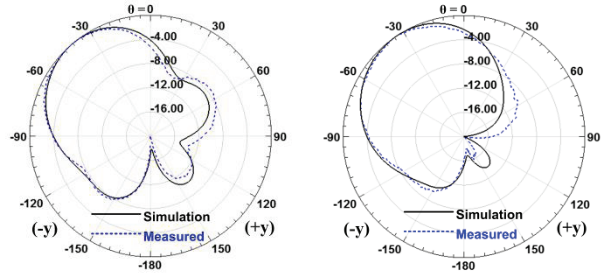

(c) (d)

Fig. 6. Simulation and measured radiation patterns for Case-I given in Table 1: (a) 1.3 GHz, (b) 1.5 GHz, (c) 1.7 GHz, and (d) 1.9 GHz.

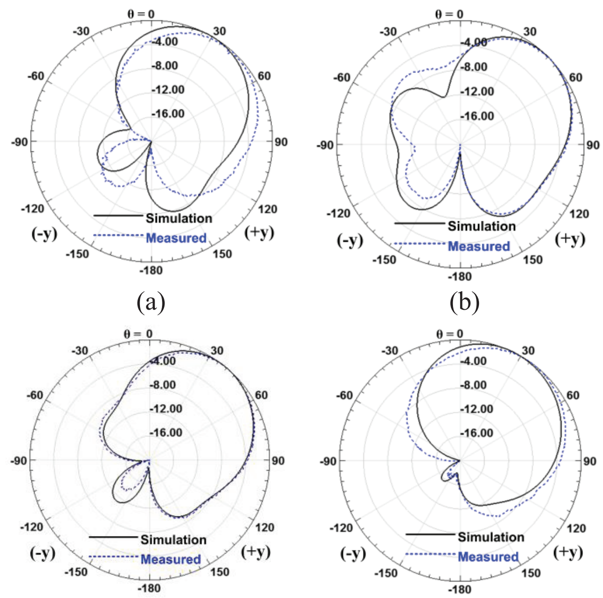

(a) (b)

(c) (d)

Fig. 7. Simulation and measured radiation patterns for Case-II given in Table 1: (a) 1.3 GHz, (b) 1.5 GHz, (c) 1.7 GHz, and (d) 1.9 GHz.

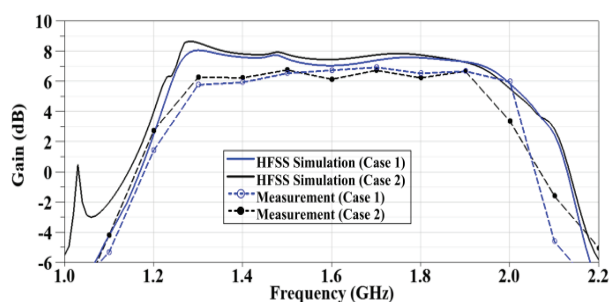

Fig. 8. A comparison of simulation and mesured antenna gain for both cases mentioned in Table 1.

In Table 2, the proposed two-element switched beam DRA structure is compared with other switched beam DRA structures found in literature. The proposed DRA structure includes only one coaxial feed and does not require any phase shifters or power splitter/combiners. The gain and overall size of proposed DRA structure is also found to be better than other reported DRA structures.

Table 2: Comparison between the proposed and other published switched beam DRAs

	No. of DRA Feeds	No. of Switchable Radiation Patterns	Impedance Bandwidth	Gain in Operating Bandwidth (dB)	Overall Size (L × W × H)
[15]	5	4 (requires power splitter/combiner)	1 MHz (58.9 -59.8 MHz)	Not mentioned	800 × 800 × 200 mm $0.16\lambda_0 \times 0.16\lambda_0 \times 0.05\lambda_0$
[16]	4	4 (requires phase shifters)	3.5 GHz (9.5 - 13 GHz)	Min: 1.5 Max: 3.0	55 × 55 × 6.8 mm $2\lambda_0 \times 2\lambda_0 \times 0.25\lambda_0$
[17]	4	4 (requires power splitter)	900 MHz (1 - 1.9 GHz)	Min: 4.5 Max: 6.5	350 × 350 × 70 mm $1.8\lambda_0 \times 1.8\lambda_0 \times 0.36\lambda_0$
Proposed DRA	1	2 (RF switches)	600 MHz (1.3 - 1.9 GHz)	Min: 6.0 Max: 7.0	235.6 × 144 × 49 mm $1.2\lambda_0 \times 0.74\lambda_0 \times 0.25\lambda_0$

λ_0 is the free space wavelength at the center frequency

V. CONCLUSION

Two elements small size wideband DRA in array configuration is proposed for beam switching applications. Dual excitation strips are utilized to excite each DRA element. Four parasitic patches associated with each DRA are utilized to increase the antenna impedance bandwidth as well as to switch antenna radiation pattern in elevation plane. Wide impedance bandwidth of approximately 37% (1.3 - 1.9 GHz) is achieved with similar radiation pattern characteristics. The antenna gain is found to be above 6 dB in the whole frequency band of operation. The proposed design based on two DRAs and a single coaxial feed network can be extended to more sophisticated antenna structures with higher gain and antenna radiation pattern reconfigurability.

ACKNOWLEDGMENT

The authors would like to extend their sincere appreciation to the Deanship of Scientific Research (DSR) at King Saud University for its funding of this research through the Research-Group Project No. RG-1436-001.

REFERENCES

[1] S. A. Long, M. W. McAllister, and L. C. Shen, "The resonant cylindrical dielectric cavity antenna," *IEEE Trans. Antennas Propagat.*, vol. 31, no. 5, pp. 406-412, May 1983.

[2] R. K. Mongia, A. Ittipiboon, and M. Cuhaci, "Measurement of radiation efficiency of dielectric resonator antennas," *IEEE Microwave and Guided Letters*, vol. 4, no. 3, pp. 80-82, 1994.

[3] A. A. Kishk, "Dielectric resonator antenna, a candidate for radar applications," *Proceedings of 2003 IEEE Radar Conference*, pp. 258-264, May 2003.

[4] I. A. Eshrah, A. A. Kishk, A. B. Yakovlev, and A. W. Glisson, "Theory and implementation of dielectric resonator antenna excited by a waveguide slot," *IEEE Trans. Antennas Propagat.*, vol. 44, no. 53, pp. 483-494, Jan. 2005.

[5] M. Khalily, M. K. A. Rahim, and A. Kishk, "Bandwidth enhancement and radiation characteristics improvement of rectangular dielectric resonator antenna," *IEEE Antennas and Wireless Propagation Letters*, vol. 10, pp. 393-395, 2011.

[6] Z. Deen, H. Saber, H. A. Malhat, and K. H. Awadalla, "8×8 near-field focused circularly polarized cylindrical DRA array for RFID applications," *Applied Computational Electromagnetics Society Journal (ACES)*, vol. 27, no. 1, 2012.

[7] A. Tadjalli, A. R. Sebak, T. A. Denidni, and A. A. Kishk, "Spheroidal dielectric resonator antenna," *URSI Digist, USNC/URSI National Radio Science Meeting*, pp. 184, 2004.

[8] A. Tadjalli, A. Sebak, T. Denidni, and I. Ahadi-Akhlaghi, "Design of elliptical dielectric resonator antennas using genetic algorithm and Rayleigh-Ritz technique," *Applied Computational Electromagnetics Society Journal (ACES)*, vol. 24, no. 1, pp. 37-44, 2009.

[9] Z. Deen, S. H. S. M. Gaber, A. M. Abd-Elhady, K. H. Awadalla, and A. Kishk, "Perforated dielectric resonator antenna reflectarray," *Applied Computational Electromagnetics Society Journal (ACES)*, vol. 26, no. 10, 2011.

[10] G. Almpanis, C. Fumeaux, and R. Vahldieck, "Novel broadband dielectric resonator antennas fed through double-bowtie-slot excitation scheme," *Applied Computational Electromagnetics Society Journal (ACES)*, vol. 22, no. 1, 2007.

[11] A. Petosa, *Dielectric Resonator Antenna Handbook*, *Artech House Publishing*, ISBN: 978-1-59693-206-7, 2007.

[12] A. Motevasselian, A. Ellgardt, and B. L. G.

Jonsson, “A circularly polarized cylindrical dielectric resonator antenna using a helical exciter,” *IEEE Trans. Antennas Propagat*., vol. 61, no. 3, Mar. 2013.

[13] A. Petosa and A. Ittipiboon, “Dielectric resonator antenna: a historical review and the current state of the art,” *IEEE Antennas Propagat. Mag*., vol. 52, pp. 91-116, Oct. 2010.

[14] H. Fayad and P. Record, “Experimental investigation on new steerable dielectric resonator antenna,” *IET Electronics Letters*, vol. 43, no. 19, pp. 1009-1010, Sep. 2007.

[15] S. P. Kingsley and S. G. O’ Keefe, “Beam steering and monopulse processing of probe-fed dielectric resonator antennas,” *IEE Proceedings-Radar, Sonar and Navigation*, vol. 146, no. 3, pp. 121-125, 1999.

[16] H. Fayad and P. Record, “Multi-feed dielectric resonator antenna with reconfigurable radiation pattern,” *Progress in Electromagnetics Research*, vol. 76, pp. 341-356, 2007.

[17] M. Grag and S. K. Sharma, “Wide-bandwidth dielectric resonator antenna with omni-directional radiation patterns for beam focusing properties in a circular array,” *International Journal of RF and Microwave Computer-Aided Engineering*, vol. 24, no. 1, pp. 92-101, 2014.

[18] R. K. Mongia and A. Ittipiboon, “Theoretical and experimental investigations on rectangular dielectric resonator antennas,” *IEEE Trans. Antennas Propagat*., vol. 45, no. 9, pp. 1348-1356, Sep. 1997.

[19] R. E. Collin and F. J. Zucker, *Antenna Theory, Part 1*, Inter-University Electronics Series, 1969.

[20] M. K. Saleem, M. A. S. Alkanhal, and A. F. Sheta, “Dual strip-excited dielectric resonator antenna with parasitic strips for radiation pattern reconfigurability,” *International Journal of Antennas and Propagation*, vol. 2014, Jan. 2014.

[21] B. Li and K. W. Leung, “Strip-fed rectangular dielectric resonator antennas with/without a parasitic patch,” *IEEE Trans. Antennas Propagat*., vol. 53, iss. 7, pp. 2200-2207, July 2005.